

# Co-treatment With the Herbal Medicine SIP3 and Donepezil Improves Memory and Depression in the Mouse Model of Alzheimer's Disease

**Quan Feng Liu**

Dongguk University

**Hoon Choi**

Seoul National University College of Pharmacy

**Taekwon Son**

Seoul National University College of Pharmacy

**Young-Mi Kim**

Seoul National University College of Pharmacy

**Suganya Kanmani**

Dongguk University

**Young-Won Chin**

Seoul National University College of Pharmacy

**Seung-Nam Kim**

Dongguk University

**Kwang-Ki Kim**

Dongguk University Ilsan Hospital

**Kyu-Won Kim**

Seoul National University College of Pharmacy

**Byung-Soo Koo** (✉ [koobs@dongguk.ac.kr](mailto:koobs@dongguk.ac.kr))

Dongguk University Ilsan Hospital <https://orcid.org/0000-0002-9077-1591>

---

## Research

**Keywords:** Alzheimer's disease, Santalum album, Illicium verum, Polygala tenuifolia, Donepezil, APPswe/PS1dE9

**Posted Date:** January 7th, 2021

**DOI:** <https://doi.org/10.21203/rs.3.rs-139699/v1>

**License:**   This work is licensed under a Creative Commons Attribution 4.0 International License.

[Read Full License](#)

**Version of Record:** A version of this preprint was published at Current Alzheimer Research on April 13th, 2022. See the published version at <https://doi.org/10.2174/1567205019666220413082130>.

# Abstract

**Background:** Alzheimer's disease (AD) is a lethal progressive neurodegenerative disorder. Currently, many acetylcholinesterase inhibitors, such as donepezil, is widely used for the treatment of AD. However, the efficacy of long-term donepezil use is limited. SIP3, a mixture of *Santalum album*, *Illicium verum*, and *Polygala tenuifolia*, a new formula derived from traditional Korean herbal medicine. In this study, SIP3 were assessed the survival of *Drosophila* AD model and synergistic effect of SIP3, donepezil co-treatment of AD using APP/PS1 transgenic mice.

**Methods:** In *Drosophila* AD models, we analyzed the survival, climbing ability and acridine orange (AO) staining. In APP/PS1 mice, at six months of age were randomized into four groups. Then, these groups were orally administered vehicle (for the control), donepezil, low and high doses SIP3 plus Donepezil respectively for six months. The passive avoidance test (PAT) and the Morris water maze (MWM) were analyzed cognitive behavioral changes. In addition, the forced swimming test (FST) and the tail suspension test (TST) were assessed depression-like behavior. To investigate the molecular and cellular mechanisms underlying positive effects of SIP3 on AD, the cerebral cortex transcriptomes were analyzed by RNA sequencing.

**Results:** Using the passive avoidance test (PAT), we analyzed the combination of SIP3 and donepezil improved the learning capabilities and memory of APP/PS1 mice, compared with the group treated with donepezil only, in late stage of AD. In addition, using the Morris water maze (MWM) test, co-treatment with donepezil and a low concentration of SIP3 significantly ameliorated cognitive impairment. Co-administration of SIP3 and donepezil effectively reduced depression-like behavior in the forced swimming and tail suspension tests. Furthermore, RNA sequencing of cerebral cortex transcriptome revealed that gene expression profiles after low dose of SIP3 co-treatment are slightly similar to those of normal phenotype mice than those obtained after donepezil treatment alone. Gene ontology (GO) along with Kyoto Encyclopedia of Genes and Genomes (KEGG) pathway have demonstrated that differentially expressed genes were involved in locomotor behavior and neuroactive ligand-receptor interactions.

**Collectively:** our results suggest that co-treatment of low dose of SIP3 and donepezil improves impaired learning, memory, and depression in late stage of AD in mice.

## Background

Alzheimer's disease (AD) is one of the most common and severe neurodegenerative diseases in elderly people [1, 2]. It is characterized by memory loss and progressive cognitive impairment. Although the pathogenesis of AD is not completely understood, it is a result of a cascade of pathological changes [2]. These changes include dysfunction of the cholinergic neurotransmission system,  $\beta$ -amyloid (A $\beta$ ) peptide aggregation, and tau-protein hyperphosphorylation, resulting in the formation of senile plaques (SP) [1, 3]. Acetylcholine (ACh), a common neurotransmitter in the central nervous system (CNS) [4] plays a crucial role in maintaining normal learning and memory. Indeed, a gradual loss of ACh has been shown to result

in impaired cognitive abilities, especially during the development and progression of AD [5]. For that reason, acetylcholinesterase inhibitors (AChEIs) are thought to be promising therapeutic drugs for the treatment of neurodegenerative diseases, such as AD and senile dementia. Currently, the AChEIs approved by the FDA for the treatment of AD are donepezil, galantamine and rivastigmine [6, 7].

Many studies have reported that donepezil alleviates the neuronal degeneration caused by damaged cholinergic neurotransmission. It has also been shown to attenuate the neural toxicity caused by A $\beta$  peptide aggregation [8]. Donepezil significantly reduces the severity of neuropsychiatric symptoms in patients with AD; however, several side effects, including gastrointestinal upset, diarrhea, slightly increased anxiety, and insomnia, have been reported [9]. In addition, its efficacy drops below baseline level after nine months. To overcome this problem of short-term efficacy, many attempts are being made to improve the long-term efficacy of donepezil in AD patients by combining it with other drugs. For example, the long-term combination of memantine with donepezil is better at slowing down perception and dysfunction in AD than the use of donepezil alone [10–12].

SIP3 is a mixture of three herbal extracts, *Santalum album* was provided by TFS Corporation Ltd (Nedlands, Australia), *Illicium verum*, and *Polygala tenuifolia* derived from traditional Korean medicine. According to Dongui Bogam, an encyclopedic source of traditional Korean medicinal knowledge and techniques including herbal folk medicine, these ingredients were often prescribed for poor memory and in the treatment of dementia.

*S. album* has anti-vasculogenic mimicry activity and vasorelaxant activity, increasing blood flow to the brain [13, 14]. The major bioactive constituent of *S. album* is santalol, which works as a neuroleptic. *I. verum* has long been used in herbal medicine to treat insomnia and inflammation [15, 16]. The major component of *I. verum*, trans-anethole, has anti-oxidant activities [17]. *P. tenuifolia* has been used as a cure for both insomnia and amnesia [18]. More recently, it has been prescribed for memory dysfunction and various brain inflammatory diseases [19].

In this study, we assessed the synergistic effects of donepezil and SIP3, as a co-treatment in an AD mouse model, and compared them with the effects seen using donepezil alone.

## Methods

### Preparation of SIP3 extract

In this study, we purchased *S. album* from TFS Corporation Ltd (Nedlands, Australia), *I. verum*, and *P. tenuifolia* from an authorized pharmaceutical company (Taegu Co., Korea), and the samples have been located in the Medicinal Herb Garden of Dongguk University for connecting reasons. A specimen *S. album* (CYWDU-KP0014), *I. verum* (CYWDU-KP0015), and *P. tenuifolia* (CYWDU-KP0013) were stored in low temperature (4 °C). Each of the three herbal extracts (100 g) was pulverized and extracted twice using 30% ethanol found in 100 °C among reflux condenser during 3 h, then was purified with a 50  $\mu$ m filter and

fixed by a lyophilizer to collect the extract at -60 °C. Following this whole procedure, the final yield was approximately 8.7 g of dried material (average yield rate is 8.7%) and was stored at -70 °C until use.

## UPLC-UV and ESI-MS analysis of SIP3

A C<sub>18</sub> column (2.1 × 150 mm, 1.7 μm, Waters, Milford, MA, USA) was used for chromatographic separation analysis. An aliquot of the test sample (2 μL) was infused into the Ultra Performance Liquid Chromatography (UPLC) scheme for assay. The adaptable stage subsisted of 0.1% formic acid in water (A) as well as 0.1% formic acid in acetonitrile (B). The mobile phase, consisting of (A) and (B), was conveyed at a discharge amount of 0.3 mL/min through the following programmed gradient elution: 10% (B, v/v) isocratic for 1 min, 10→30% (B) in 19 min, 30→50% (B) in 10 min, 50→100% (B) in 10 min, 100% (B) isocratic for 3 min, 100→10% (B) in 0.5 min, 10% (B) isocratic for 4.5 min as post-run for reconditioning. The column temperature was maintained at 40 °C. Mass spectrometer (Xevo G2 Q-TOF MS, Waters) equipped with the electrospray ionization (ESI) was operated in the negative ion mode. Capillary voltage and cone voltage were set at 3.0 kV and 40 V, respectively. Gas flow rates for cone and desolvation gas were set at 50 L/h and 600 L/h, respectively. Source temperature and desolvation temperature were set to 50°C and 350°C, respectively. Mass spectral data were recorded in the range of *m/z* 50-1800. UPLC-Mass spectrometry was performed per the aforementioned method. The SIP3 stock solution was prepared by dissolving the accurately weighed substances in methanol-water (50:50, v/v).

## *Drosophila* AD models

To develop *Aβ42*-overexpressing flies, we handling the UAS-GAL4 scheme. In this scheme, the organizer has guiding the explanation of yeast transcriptional stimulator GAL4. Then the GAL4 stimulates the target gene containing UAS, which carried GAL4 binding sites (Phelps and Brand, 1998). The *GAL4* gene is fixed near a tissue-special organizer, permitting ectopic expression of the specific gene in the desired tissue. For example, embryonic lethal aberrant view-*GAL4* (*elav-GAL4*) and glass multimer announcer-*GAL4* (*GMR-GAL4*) absolute target gene exposition in the neurons as well as the progressing eye, respectively.

The wild-type (*w<sup>1118</sup>*) strain, glass multimer reporter-*GAL4* (*GMR-GAL4*; eye driver), embryonic lethal aberrant vision-*GAL4* (*elav-GAL4*; pan-neuronal driver), and *UAS-Aβ42* were received from Bloomington *Drosophila* Stock Center (Bloomington, USA). All flies were maintained with cornmeal-bean powder, yeast-agar standard medium at 25 °C. The genotypes of *Drosophila* strains were control (*w<sup>1118</sup>*), *GMR-GAL4* (*GMR-GAL4/GMR-GAL4*), *GMR > Aβ42* (*GMR-GAL4, UAS-Aβ42/GMR-GAL4, UAS-Aβ42*), *elav-GAL4* (*elav-GAL4/elav-GAL4*), and *elav > Aβ42* (*UAS-Aβ42/UAS-Aβ42, elav-GAL4/elav-GAL4*).

## Analysis of *Drosophila* development

One-hundred embryos placed by means of genotype moved up in allowed media were collected on grape juice agar plates. These embryos were transmitted to accepted fly media with or without SIP3 extract, and increased at 25 °C in upright accepted plastic shell vials. Fifty-planned larvae were continued per vial. The amounts of enclosed adult flies were counted.

## Climbing assay

Ten male flies were gathered in the mounting ability approval vials. Then, the flies were incubated for 1 h at the room temperature being acclimatization. To calculate the moving capability, the flies were lightly knocked down to the base of the standard vial, the amount of flies, which moved to the roof of the vial 8 sec in advance, was recorded. Ten trials were achieved for particular batch. Moving capabilities (ratio of the number of flies that climbed to the top against the total number of flies) were documented for various associations, as well as mean mounting skills for 10 duplicated tests was correlated such control flies. All mounting diagnoses were observed at 25 °C.

## Acridine orange staining

The brains or eye imaginal discs has connected with *Drosophila* stage L3 larvae were divided in phosphate-buffered saline (PBS). The tissues were treated for 5 min in  $1.6 \times 10^{-6}$ M acridine orange solution (Sigma-Aldrich, USA), and briefly washed with PBS. The elements were checked on the bottom of Axiophot2 fluorescence microscope (Carl Zeiss, Germany).

## Mouse AD model

The present study was approved by the Animal Care and Ethical Committee of Dongguk University (Clinical trial approval number IACUC-2017-011-1). All animal handling procedures followed the guidelines of Institute for Laboratory Animal Research of the Dongguk University. APP<sup>swe</sup>/PS1<sup>dE9</sup> (APP/PS1) transgenic mice overexpressing human mutated APP and PS1 were purchased from the Jackson Laboratory (Bar Harbor, ME, USA). The animals were accommodated under laboratory settings at a composed temperature ( $20 \pm 2$  °C) as well as preserved the bottom of the light–dark cycles, 12 h of individually (from 07:00 to 19:00 h) among food as well as water made available ad libitum. APP/PS1 mice at six months of age were randomized into control (n = 5), SIP3 with Donepezil (n = 5) and Donepezil alone (Eisai Korea, Inc.) (n = 5). Lab chow containing SIP3 with Donepezil or Donepezil alone was prepared for a mouse to have SIP3L (100 mg/kg/day) and SIP3H (300 mg/kg/day) or donepezil (0.1 mg/kg/day) [20]. The mice were fed lab chow containing SIP3 with Donepezil or Donepezil alone for six months beginning at six months of age.

## Step-through passive-avoidance test

The device (AP model; O'Hara Co., Tokyo, Japan) for the step through passive-avoidance test subsisted of two chambers, illuminated chamber [100 mm × 120 mm × 100 mm; light at the top of chamber (27 W, 3000 lx)] and dark chamber (100 mm × 170 mm × 100 mm). The chambers were specific through a guillotine door. In the time of learning stage, a mouse was located in the illuminated intact chamber. As

the chamber was lit, the mouse walked into the exposed guillotine door into the dark chamber. The time consumed in the illuminated chamber was characterized as the latency time. Three seconds later, the mouse arrived the dark chamber, a foot agitate (0.3 mA, 50 V, 50 Hz ac, for 3 s) was expressed to the floor grids in the dark chamber. The mouse kept escape against the shock only by moving back to the intact illuminated chamber. Similar addition trials as the learning stage were moved out at 12 months of age. It was considered as training avoidance from foot-agitate if the mouse continued in the illuminated chamber for 300 s after being located there. The detention trials were moved out 24 h after training trial to evaluate the avoidance memory. The latency time was analyzed for the capable of 300 s without conveying foot agitate. It was concluded that the mouse maintained the avoidance memory when it continued in the illuminated intact chamber for 300 s.

## **Morris water maze test**

This behavioral analyses was achieved at 12 months of age. Water was made with milky white ink, and the temperature was 22 ~ 25 °C. The diameter and the height of the water maze model were 100 as well as 35 cm, respectively. A transparent acrylic plastic platform was immersed 1 cm below the water. During this trainings, test mice were located in the water and permitted 120 s to check being the platform. Mice were permitted 10 s to stay on the platform and then recurred to the home cage. A video camera was seated on the ceiling over the pool and was associated to a video recorder as well as tracking equipment (Ethovision XT, Noldus, VA, USA), allowing on- and offline automatic tracking of the direction seized by the mouse.

## **Forced swimming test**

Mice were located in a Plexiglas cylinder, 25 cm in height among a 15 cm inner diameter, accomodating water at a temperature of  $25 \pm 1$  °C and a bottom of 10 cm so they could not escape and touch the bottom. Water was replaced among various swim session to inhibit possible things of an alarm object discharged by mice as the swim session. There were two swim sessions. The first was a 15 min pre-test swim during 3 days in a row and a second 5 min swim test. The pre-test helps the improvement of immobility over the test period and boosts the sensitivity for recognizing antidepressant behavioral effects. The 5 min swim test was used to analyze the behavior of the mice such as swimming, climbing, and immobility.

## **Tail suspension test**

Mice both acoustically as well as prominently isolated were depended individually by their tails 40 cm beyond the tabletop among the use of an adhesive tape located roughly 1 cm from the tip of the tail. Subsequently a few minutes of vigorous movement, the mice hung passively and absolutely motionless. The total immobility stage in amount of seconds was calculated over the 6 min test. Mice were examined immobile among the absence of any limb or body developments, except for those generated over respiration. A decrease in the period of immobility is suggestive of an antidepressant-like effect.

## **Corticosterone levels**

Serum was isolated by centrifugation at  $3,000 \times g$  for 15 min at 4 °C immediately after trunk blood collection and was kept at -80 °C. Serum corticosterone levels were quantified in duplicate using an enzyme-linked immunoassay (ADI-900-097, Enzo Life, NY, USA) according to the manufacturer's instructions.

## **mRNA sequencing**

Total RNA was isolated from the brain tissue of mice (cortex) accepting TRIzol® RNA Isolation Reagents (Life technologies, Carlsbad, CA, USA). RNA purity was proved by a bioanalyzer accepting an Agilent RNA 6000 Pico Kit (Agilent, Santa Clara, CA, USA). The isolated total RNA was handled for adapting mRNA sequencing library accepting TruSeq stranded mRNA sample measuring kit (Illumina, San Diego, CA, USA) according to manufacturer's instruction. Simply, mRNAs were screened from 400 ng total RNA by RNA purification bead accepting polyA capture, and pursued through enzyme shearing. After first and second strand cDNA synthesis, A-tailing as well as end repair were completed for ligation of proprietary primers that integrate unique sequencing adaptors along index for tracking illumina reads taken away from multiplexed samples run on a single sequencing lane. For each library, an insert size of approximately 220 bp was accepted by Bioanalyzer accepting an Agilent DNA Kit (Agilent, Santa Clara, CA, USA) and the density of library was analyzed by real-time PCR using CFX96 real time system (BioRad, Hercules, CA, USA). Samples were sequenced along the Illumina NextSeq 500 platform, among paired-end, 75-bp reads for mRNA-seq accepting the NextSeq 500/550 High Output Kit version 2 (for 150 cycles). The raw image data was converted by base-calling into sequence data and was stored in FASTQ format.

## **NanoString nCounter Platform**

The RNA samples were run on the NanoString nCounter Analysis System (NanoString Technologies, Inc., WA, USA) according to the manufacturer's directions. 5 µL (100–300 ng) of each RNA sample was mixed with 8 µL of the Master Mix (reporter codeSet and hybridization buffer). 2 µL of the capture probeSet was added; the solution was mixed and spin down. It was placed in a 65 °C thermocycler (Bio-Rad Laboratories Inc, Hercules, California, USA) for 16 hours (Maximum hybridization time should not exceed 48 hours). The samples were transferred to the preparation station (NanoString Technologies, Seattle, WA) with prepared nCounter Master Kit and a cartridge. The preparation station 12 lanes per run in approximately 2.5 to 3 hours. The cartridges were transferred to the Digital Analyzer (NanoString Technologies, Seattle, WA) for analysis. Cartridges were then scanned on the Digital Analyzer at 555 fields of view.

## **RNA preparation and quantitative real-time reverse transcription-polymerase chain reaction**

As long as the quantitative real-time reverse transcription-polymerase chain reaction (qRT-PCR) analyses, the total mRNA from three mouse brain cortex was filtered with TRIzol reagent (Thermo Fisher Scientific, USA). Then, cDNA was synthesized with cDNA Synthesis Master Mix (LeGene Biosciences, USA), and

primers for genes (Table 1) and qRT-PCR was performed with SYBR Green PCR Master Mix (Thermo Fisher Scientific, USA) and a StepOne Realtime PCR system (Thermo Fisher Scientific, USA). The relative level of *Gfap*, *Il1a*, *Irs2*, *Nos3*, *Tgfbr2*, *Nefh*, and *Gapdh* mRNA to tubulin mRNA was statistically analyzed using Student's t-test.

## Data analysis

Current assay was quantitatively analyzed for statistical significance accepting either a Student's *t*-test (two-tailed) or a one-way ANOVA pursued by a Tukey-Kramer multiple correlations test. Student's *t*-test was adapted for correlations of two associations. SPSS (ver. 19, Somers, USA) software was used, and  $P < 0.05$  designated a significant difference.

## Trimming, alignment, and expression analysis

Five paired-end 75 bp reads of mouse sample were cut down for both PCR and sequencing adapters with Cutadapt. Trimmed reads were regulated to the mm10 mouse reference genome using STAR.

Quantification of gene expression was observed with Cufflinks to measure FPKM values. Presence of significant differential expression was determined with Cuffdiff at gene level. Heatmap of gene differential expression was generated using R language. Functional classification was performed using DAVID.

## Gene set enrichment analysis

Gene set enrichment analysis (GSEA) was used to determine the extent to which expression profiles were enriched for a priori defined sets of genes from biologically coherent pathways. GSEA was performed using version 2.2 of GSEA run on all the gene sets in version 5.2 of the Molecular Signatures Database and to correct for multiple hypotheses testing; the FDR threshold was set at  $\leq 0.25$ . A list of the specific signatures used for graphical representation and their specific description has been added to the Excel file with raw data.

## Quantifying miRNA expression and differential expressed miRNA analysis

To quantify the miRNA expression values, first background correction and normalization used default options with control probes in each Codeset. Second, differentially expressed miRNAs between the two selected biological conditions were analyzed by t-test on log<sub>2</sub>-transformed count data. Background correction and normalization, differential expression analysis was performed with nSolver Analysis software ver 4.0. Comparative analysis between groups was performed using *P* value and fold-change values. *P* values were determined by Student's t-test for assessing the significance of differences between experimental groups. False discovery rate (FDR) was controlled by adjusting *P* value using *Benjamini-Hochberg* algorithm. After adjusting, statistical significance was set to  $P < 0.05$ . Visualization of differentially expressed genes was conducted using R statistical language v. 3.1.2. Furthermore, Kyoto Encyclopedia of Genes and Genomes (KEGG) pathway enrichment analysis was performed.

## Results

# SIP3 Exerts with donepezil ameliorated $A\beta 42$ -induced neurological phenotypes of *Drosophila* AD models

Initially, we found that SIP3 contains oligosaccharide ester-type and saponin-type compounds, such as Tenuifoliside B and E, Onjisaponin A-F, and Tenuifoliose A (Fig. S1). Saponins are known to have significant neuroprotective effects by attenuating various central nervous system disorders such as stroke, AD, Parkinson's disease, and Huntington's disease [21].

To analyze whether SIP3 or SIP3 with donepezil exerts toxicity against the organism, we tested the effect of SIP3 or SIP3 with donepezil intake on the development of *Drosophila*. As shown in Fig. 1a, survival of flies fed with 50  $\mu\text{g}/\text{mL}$  *S. album*, *I. verum*, and *P. tenuifolia* used separately and SIP3, donepezil alone or SIP3 with donepezil did not show any difference as compared to that of control, which suggests that *S. album*, *I. verum*, *P. tenuifolia*, SIP3 or donepezil alone and SIP3 with donepezil did not exert prominent toxic effect at these doses. As compared to the control, SIP3 or SIP3 with donepezil significantly increased the survival of  $A\beta 42$ -expressing AD flies *elav* >  $A\beta 42$  (*UAS-A\beta 42/UAS-A\beta 42; elav-GAL4/elav-GAL4*) (Fig. 1b). In addition, the absorption of the SIP3L (co-administration among donepezil and a lesser concentration of SIP3 extract 50  $\mu\text{g}/\text{mL}$ ) or SIP3H (co-administration among donepezil and a huge concentration of SIP3 extract 200  $\mu\text{g}/\text{mL}$ ) among donepezil (0.1  $\mu\text{g}/\text{mL}$ ) increased motor activity of pan-neuronally  $A\beta 42$ -expressing AD flies *elav* >  $A\beta 42$  (*UAS-A\beta 42/UAS-A\beta 42; elav-GAL4/elav-GAL4*) (Fig. 1c). Later, we investigated the neuroprotective cause of SIP3 among donepezil applying  $A\beta 42$ -suggesting *Drosophila* AD models. When  $A\beta 42$  was carried in the proceeding of eyes *GMR* >  $A\beta 42$  (*GMR-GAL4, UAS-A\beta 42/GMR-GAL4, UAS-A\beta 42*), eye reduction and deterioration, was investigated to that of control flies *GMR-GAL4* (*GMR-GAL4/GMR-GAL4*) (Fig. 1d). The  $A\beta 42$ -induced defective eye phenotype was prominently suppressed by intake of the 50 and 200  $\mu\text{g}/\text{mL}$  SIP3 with donepezil extract (Fig. 1d). Additionally,  $A\beta 42$ -induced the cell death in the eye imaginal disc along with suppressed by the intake of SIP3 with donepezil extract (Fig. 1d bottom panels). Moreover, intake of SIP3L with donepezil than donepezil alone was strongly suppressed  $A\beta 42$ -induced cell death in larval brain (Fig. 1e).

## Treatment with a combination of SIP3 and donepezil improves learning and memory in the late stage of APP/PS1 mice

To examine the therapeutic effect of the combination of SIP3 and donepezil in AD, we used normal (NOR) and APP/PS1 transgenic mice without (CON) or treated with donepezil in the absence (DON) or presence of a low or high concentration of SIP3 (SIP3L or SIP3H, respectively) for 6 months (Fig. 2) [22]. There were no significant differences in body weight changes (Fig. S2a), food intake (Fig. S2b), or the food efficiency ratio (FER; Fig. S2c) between the groups during the experimental period.

To assess the effect of SIP3 on learning and memory in the early and late stages of AD, we conducted the passive avoidance test (PAT), initially at Day 0, and thereafter once monthly for 6 months (Fig. 2a). In this test, the animals learn to avoid an environment in which an unpleasant stimulus has previously been delivered. In the training phase, a mouse is placed in the bright chamber of a 2-chamber box, receiving an electronic foot-shock when it passes through the dark chamber, the environment that it would usually favor. After 24 hours, the mouse is again placed in the bright chamber. Mice with normal learning and memory avoid entering the dark chamber, where they were previously shocked, and this translates to a higher latency value. After one month of dosing, donepezil-treated (DON) mice had slightly higher latency values than the SIP3L or SIP3H-treated mice (Fig. 2b); however, after this, at months 5 and 6, those in the SIP3L and SIP3H groups had significantly improved learning and memory compared with those in the CON or DON groups (Fig. 2c). These results suggest that SIP3 and donepezil co-treatment improves the long-term memory of APP/PS1 mice.

## **Administration of SIP3L and donepezil significantly improves the cognitive abilities of APP/PS1 mice**

To confirm whether SIP3 treatment improves cognitive dysfunction in the late dementing stage of AD and to study spatial learning and memory, we performed the Morris water maze (MWM) test (Fig. 3a) [23]. In the training phase, we observed on the first day that mice in all groups had similar escape latencies (Fig. 3a). However, on Day 4, the escape latency of the SIP3L mice, but not of the SIP3H mice, was significantly reduced, compared with that of the CON or DON mice (Fig. 3a). Notably, in the post-training probe phase, SIP3L mice displayed a comparable escape latency to that of the NOR mice (Fig. 3b). Furthermore, compared with CON or DON mice, SIP3L mice took less time to reach the target quadrant (platform in Zone 1 location opposite Zone 3 and right/left adjacent Zone 2, Zone 4) (Fig. 3c), and the time spent in the target quadrant was significantly increased (Fig. 3d). These results confirm that, in this mouse model, SIP3L treatment may ameliorate the cognitive impairment seen in spatial learning and memory function in the late dementing stage of AD.

## **SIP3 and donepezil co-treatment improves depression and anxiety in APP/PS1 mice**

Depression is very common among people with AD, and it has a substantial impact on the development and progression of AD. The forced swimming test (FST) as well as the tail suspension test (TST) were used to calculate the tendency towards depression-like behavior in the mice (Fig. 2a) [24]. Both tests are based on the observation that, when subjected to an extreme situation from which it cannot escape, a mouse will cease attempts to escape and become immobile. A depressed mouse will cease activity for a longer period than a normal mouse. In the FST, there was no difference between CON and DON mice in immobility time (Fig. 4a). However, the immobility times of the SIP3L or SIP3H mice were significantly lower than those of the CON and DON mice (Fig. 4a). This phenomenon was also observed in the TST, in which the immobility times of the SIP3L or SIP3H mice were significantly reduced compared with those

of the CON and DON mice (Fig. 4b). Furthermore, as depression is highly correlated with elevated corticosterone levels in serum, we compared the corticosterone levels between the groups. Although there was no difference in serum corticosterone levels between the CON and DON mice, the levels were significantly reduced in the SIP3L and SIP3H mice compared with those in the CON and DON mice (Fig. 4c). In particular, SIP3L mice remarkably reduced the serum corticosterone level. These findings indicate that SIP3 co-treatment with donepezil effectively ameliorates depression-like behavior in APP/PS1 mice.

## **Deep sequencing identified changes in the transcriptome of the SIP3L APP/PS1 mice**

To examine the molecular as well as cellular mechanisms underlying the positive effects of SIP3 on AD, the cerebral cortex transcriptomes of the NOR, CON, DON, SIP3L, and SIP3H mice were analyzed by RNA sequencing (RNA-seq). A total of 64 genes were found to be differentially indicated between the CON and SIP3L mice (Cuffdiff with  $FDR \leq 0.05$ ). Of the 64 differentially expressed genes, 42 genes were upregulated, and 22 were downregulated, in the mice in the SIP3L group (Fig. 5a). Furthermore, of the 42 differentially upregulated genes, simple overlap analysis revealed that 28 genes overlapped between the SIP3L and DON treatments, but that 14 genes were exclusively upregulated by the SIP3L co-treatment (Fig. 5b). Conversely, of the 22 differentially downregulated genes, 10 genes overlapped between the DON and SIP3L treatments, but 12 genes were downregulated only by the SIP3L co-treatment (Fig. 5b). Therefore, we found that several genes are specifically regulated by SIP3L and could probably be associated with antidepressant or memory cognition. The gene expression profiles revealed that SIP3L co-treatment results in a phenotype closer to that of the normal mice than that seen after DON treatment alone (Fig. 5a). In agreement with the SIP3L results from the PAT and MWM tests, the expression of genes belonging to the gene ontology (GO) terms, “locomotory behavior”, “neuropeptide signaling pathway”, “visual learning”, and “response to calcium ion”, were mostly altered in the SIP3L group (Fig. 6a). In addition, Kyoto Encyclopedia of Genes and Genomes (KEGG) pathways, such as the calcium signaling pathway (mmu04020), cocaine addiction (mmu05030), and morphine addiction (mmu05032), were also mostly affected by the SIP3L co-treatment (Fig. 6b) [25]. To compare SIP3L co-treatment with DON treatment alone, we conducted gene set analysis between DON and SIP3L mice. The expression of mRNAs belonging to the gene ontology (GO) terms, “flavonoid glucuronidation” and “flavonoid biosynthetic process”, were mostly altered in the SIP3L group (Fig. 6c). The flavonoids are known to exert a neuroprotective effect [26]. In addition, Kyoto Encyclopedia of Genes and Genomes (KEGG) pathways, such as the neuroactive ligand-receptor interaction (mmu04080), cytokine-cytokine receptor interaction (mmu04060), and Pentose and glucuronate interconversions (mmu00040), were also mostly affected by the SIP3L co-treatment (Fig. 6d). Furthermore, to investigate the molecular mechanisms of transcriptional regulation underlying the positive effects of SIP3 on AD, the cerebral cortex small RNA transcriptomes of the NOR, CON, DON, and SIP3L mice were analyzed by small RNA sequencing (Nanodrop).

## **Pattern of miRNA was changed in the brain of SIP3L APP/PS1 mice**

Also, miRNAs in the brain were tested by microarray analysis. Overall, 147 miRNAs were significantly different between groups ( $P < 0.05$ ), and only they were considered for further analysis (Fig. 7a). Notably, the miRNA expression profiles revealed that SIP3L co-treatment results in a phenotype reversed higher than that seen after DON treatment alone, compared to CON (FC  $> 2$  or  $< -2$ , P value  $< 0.05$ ,  $n = 3$ , respectively) (Fig. 7b). miRNA-target enrichment of the differentially expressed miRNAs, revealed a list of 12 genes that were significantly associated with differentially expressed miRNAs. The twelve significant targets are presented in Fig. 7c. Among these genes, *Micall1*, *Wnt7b*, *Tmem88* were target genes are known to be associated with AD [27, 28]. Collectively, these results suggest that SIP3L co-treatment improves memory and learning abilities in the mouse AD model by modulating abnormally expressed genes during the development and progression of AD.

## Validation of differentially expressed genes identified by deep sequencing by qRT-PCR

To validate the RNA-seq data, we analyzed the expression of six randomly selected genes among 64 differentially expressed genes between the CON and SIP3L mice, *Gfap*, *Il1A*, *Irs2*, *Nos3*, *Tgfbr2*, and *Nefh* by qRT-PCR. Consistent with the RNA-seq data, the expression of all six genes was downregulated by the SIP3L co-treatment (Fig. 8). Notably, *Gfap* (Fig. 8a), *Nos3* (Fig. 8d), and *Tgfbr2* (Fig. 8e) expression levels were significantly reduced in the SIP3L group, compared with those in the DON group, these three genes have been implicated in the pathogenesis of AD. While *Il1A* (Fig. 8b), *Irs2* (Fig. 8c), and *Nefh* (Fig. 8f) expression levels were not significantly changed. These results suggest that SIP3L co-treatment effectively represses the expression of genes related to the development and progression of AD.

## Discussion

Since the pathogenesis of AD is caused by complex and multiple factors, it is reasonable to prescribe a combination of drugs with different pharmacological activities for AD patients, rather than a single drug [29–31]. In fact, it has been reported that donepezil, an AChEI, is widely prescribed for patients with moderate to severe AD, and that although it is highly effective during the early administration period, it is somewhat less effective during the later administration period [32, 33]. Here, we demonstrated that co-treatment with donepezil and a mixture of three herbal extracts, SIP3, results in improved pharmacological activity in the late dementing stage in AD mouse model, in comparison with donepezil alone.

Originally this study, was boost up higher cell viability as well as donepezil in SH-SY5Y (Neuroblastoma cell line) cells, and progressed a combo of herbal extracts SIP3. Initially 33 medicinal herbs in SH-SY5Y cells were isolated them for A $\beta$  toxicity [34]. Among them *Santalum album*, *Polygala tenuifolia*, *Illicium verum* were the perfect herb [22, 35, 36]. After evaluated the neuroprotective effect of SIP3 with donepezil using *Drosophila* AD models. *Drosophila* was a well-developed genetic and cell biological system has been examining neurodegenerative disease [37]. *S. album*, *I. verum*, and *P. tenuifolia* separately and also mixed (SIP3) together or SIP3 with dopepezil analyzed the neuroprotective effect against A $\beta$ 42 toxicity in

*Drosophila*. The survival rate was significantly increased during the combination of SIP3 and donepezil, compared to the group in which donepezil only. Also, the intake of SIP3 with donepezil significantly improved locomotive dysfunction and strongly suppressed  $A\beta_{42}$ -induced cell death. These results suggest that SIP3 with donepezil is effective for protecting the cells from  $A\beta_{42}$  cytotoxicity and neuronal functions [15].

Then, we investigated the effects of donepezil and SIP3 co-treatment on learning and memory in the APP/PS1 AD mouse model, in comparison with donepezil alone, using the PAT methodology [38, 39]. In the early stage of dementia (1 to 3 months), both treatments resulted in improved memory when compared to control mice, with no noticeable difference seen between the two groups. However, in the later stage of dementia (5 to 6 months), memory was significantly improved in the group co-treated with SIP3 than that in the group treated with donepezil alone. Based on these results, we conducted MWM test on animals at the late stage of dementia to compare cognitive abilities between the two groups [40]. In the SIP3L co-treatment group, the time to reach the target quadrant was shorter and the time spent in the target quadrant was longer, indicating that the animals in this group had a more improved cognitive ability than those treated with donepezil alone [41, 42].

During that time AD patients are well known to progress depression, which affects the development and progression of AD, we have regulated FST as well as TST experiments through study depression-like behavior in AD animals [43]. In contrary the donepezil alone group, depression was significantly enhanced in the SIP3 and donepezil co-treatment group. In addition, co-administration of SIP3 and donepezil inhibited the increase in corticosterone levels seen in the serum of the AD animals. In this study we have implemented that the SIP3 was ready to regulate serum corticosterone level in APP/PS1 mice. The outcomes were carried both peripheral and central origins over a direct action of SIP3 on adrenal glands and hypothalamic-pituitary-adrenal axis respectively. In contrary, the relationship between memory performance and corticosterone level in APP/PS1 was approved the damaging effects on memory [44]. In addition, a long term depression has influenced the spatial memory [45].

These results suggest that SIP3 and donepezil co-treatment could improve some side effects, such as anxiety and insomnia, reported in donepezil-treated AD patients.

MicroRNA is small nucleic acids consisting of about ~ 20 nucleic acids, which involved in various biological pathways, and recent studies have reported that miRNA plays a key role in neurological diseases. In this study, we found that the expressions of miRNAs were reversed its abnormal changes by DON and SIP3L cotreatment, including miRNA-15a, -27a, 32, which are linked with inflammation or apoptosis pathways [46–49], indicating that the therapeutic mechanism of SIP3 and DON might underlie miRNA regulation. Further studies are required to unravel the detailed mechanism.

RNA-seq was used to study gene expression profiles in relation to the improved cognitive ability seen in the SIP3 co-treated AD animals. Genes involved in exercise behaviors, the neuropeptide signaling pathway, and visual learning were differentially expressed in the mice of the SIP3L group in comparison to those expressed in the AD control mice. These results are consistent with the improved learning and

memory seen in the animals of the SIP3L group. Noticeably, the gene expression profiles in the SIP3L group were more similar to those of normal mice than those of the control APP/PS1 mice, those treated with donepezil alone, or those co-treated with donepezil and SIP3H. In this study, we found that co-treatment of low dose of SIP3 and donepezil can improve impaired learning, memory, and depression.

## Conclusion

We found that the co-treatment with donepezil and SIP3 was more effective than donepezil-alone in improving learning and memory capabilities in the later stages of dementia in the AD mouse model. Intriguingly, the low concentration of SIP3 and donepezil co-treatment significantly improved the cognitive abilities of AD mice. Furthermore, the co-treatment of SIP3 and donepezil showed an improved antidepressant effect. Therefore, these results demonstrate the synergistic effect of SIP3 and donepezil on symptoms of AD. Accordingly, we suggest that co-administration of SIP3 and donepezil could be a novel therapeutic strategy for the treatment of AD patients.

## Abbreviations

AD: alzheimer's disease; APP/PS1: APP<sup>swe</sup>/PS1<sup>dE9</sup>; AO: acridine orange; ACh: acetylcholine; CNS: central nervous system; AChEis: acetylcholinesterase inhibitor; *S. album*: *Santalum album*; *I. verum*: *Illicium verum*; *P. tenuifolia*: *Polygala tenuifolia*; SIP3: mix of *S. album*, *I. verum* and *P. tenuifolia*; UPLC: ultra performance liquid chromatography; PBS: phosphate-buffered saline; FER: feed efficiency ratio; PAT: passive avoidance test; MWM: morris water maze; FST: forced-swim test; TST: tail suspension test; NOR: normal; CON: control; SIP3L: co-treated with donepezil and a low concentration of SIP3 extract; SIP3H: co-treated with donepezil and a high concentration of SIP3 extract; DON: donepezil; ESI: electrospray ionization; GO: gene ontology; KEGG: kyoto encyclopedia of genes and genomes; GSEA: gene set enrichment analysis

## Declarations

### Ethics approval and consent to participate

All animal treatment and experiments were approved by the Experimental Animal Administration Committee of Dongguk University (protocol number: IACUC-2017-011-1).

### Consent for publication

All the participating authors read the manuscript and give consent for publication

### Availability of data and materials

The datasets analyzed during the current study are available from the corresponding author on reasonable request

## Competing interests

The authors declare that they have no competing interests.

## Funding

The project design, materials, data interpretation, and writing are supported by the National Research Foundation of Korea (NRF) funded by the Ministry of Education (2016R1D1A1B03932530) to B.S.K. and Midcareer Researcher Program (2018R1A2B6001590) through the National Research Foundation of Korea (NRF) funded by the Ministry of Education to K.W.K.

## Authors' contributions

Q.F.L., Y.W.C., K.K.K., K.W.K., and B.S.K. designed the experiments. Q.F.L., H.C., Y.M.K., Y.O., J.J., Y.W.C., and B.S.K. performed the experiments and conducted data analysis. T.S. and S.N.K performed the bioinformatics analysis. Q.F.L., H.C., T.S., S.J.S., S.K., K.W.K., and B.S.K. wrote the manuscript. All authors read and approved the last version of the manuscript.

## Acknowledgments

We would like to thank all laboratory staff involved in this study.

## References

1. Hardy J, Selkoe DJ. The amyloid hypothesis of Alzheimer's disease: progress and problems on the road to therapeutics. *Science*. 2002; 297(5580):353-6.
2. Wirths O, Multhaup G, Bayer TA. A modified  $\beta$ -amyloid hypothesis: intraneuronal accumulation of the  $\beta$ -amyloid peptide – the first step of a fatal cascade. *J Neurochem*. 2004;91(3):513-20.
3. Selkoe DJ. The cell biology of beta-amyloid precursor protein and presenilin in Alzheimer's disease. *Trends Cell Biol*. 1998;8(11):447-53.
4. Picciotto MR, Higley MJ, Mineur YS. Acetylcholine as a neuromodulator: cholinergic signaling shapes nervous system function and behavior. *Neuron*. 2012; 76(1):116-29.
5. Lleo A. Current therapeutic options for Alzheimer's disease. *Curr Genom*. 2007;8(8):550-8.
6. Grutzendler J, Morris JC. Cholinesterase inhibitors for Alzheimer's disease. *Drugs*. 2001;61(1):41-52.
7. Mehta M, Adem A, Sabbagh M. New acetylcholinesterase inhibitors for Alzheimer's disease. *Int J Alzheimers Dis*. 2012;2012:728983.
8. Mattson MP. Pathways towards and away from Alzheimer's disease. *Nature*. 2004;430(7000):631-9.
9. Cummings JL, McRae T, Zhang R. Effects of donepezil on neuropsychiatric symptoms in patients with dementia and severe behavioral disorders. *Am J Geriatr Psychiatry*. 2006;14(7):605-12.
10. Mangialasche F, Solomon A, Winblad B, Mecocci P, Kivipelto M. Alzheimer's disease: clinical trials and drug development. *Lancet Neurol*. 2010;9(7):702-16.

11. Molino I, Colucci L, Fasanaro AM, Traini E, Amenta F. Efficacy of memantine, donepezil, or their association in moderate-severe Alzheimer's disease: a review of clinical trials. *Sci World J*. 2013;2013:925702.
12. Zhu CW, Livote EE, Scarmeas N, Albert M, Brandt J, Blacker D, Sano M, Stern Y. Long-term associations between cholinesterase inhibitors and memantine use and health outcomes among patients with Alzheimer's disease. *Alzheimers Dement*. 2013;9(6):733-40.
13. Guan YY, Luan X, Lu Q, Liu YR, Sun P, Zhao M, Chen HZ, Fang C. Natural Products with Antiangiogenic and Antivasculogenic Mimicry Activity. *Mini Rev Med Chem*. 2016;16(16):1290-302.
14. Liu P, Kong M, Yuan S, Liu J, Wang P. History and experience: a survey of traditional chinese medicine treatment for Alzheimer's disease. *Evid Based Complement Alternat Med*. 2014;2014:642128.
15. Liu QF, Lee, JH, Kim YM, Lee S, Hong YK, Hwang S, Oh Y, Lee K, Yun HS, Lee IS, Jeon S, Chin YW, Koo BS, Cho KS. In Vivo Screening of Traditional Medicinal Plants for Neuroprotective Activity against Abeta42 Cytotoxicity by Using *Drosophila* Models of Alzheimer's Disease. *Biol Pharm Bull*. 2015;38(12):1891-901.
16. Wang GW, Hu WT, Huang BK, Qin LP. *Illicium verum*: a review on its botany, traditional use, chemistry and pharmacology. *J Ethnopharmacol*. 2011;136(1):10-20.
17. Bhadra S, Mukherjee PK, Kumar NS, Bandyopadhyay A. Anticholinesterase activity of standardized extract of *Illicium verum* Hook. f. fruits. *Fitoterapia*. 2011;82(3):342-6.
18. Buccafusco JJ. Multifunctional receptor-directed drugs for disorders of the central nervous system. *Neurotherapeutics*. 2009;6(1):4-13.
19. Li Z, Liu Y, Wang L, Liu X, Chang Q, Guo Z, Liao Y, Pan R, Fan TP. Memory-Enhancing Effects of the Crude Extract of *Polygala tenuifolia* on Aged Mice. *Evid Based Complement Alternat Med*. 2014;2014:392324.
20. Romberg C, Mattson MP, Mughal MR, Bussey, TJ, Saksida LM. Impaired attention in the 3xTgAD mouse model of Alzheimer's disease: rescue by donepezil (Aricept). *J Neurosci*. 2011;31(9):3500-7.
21. Fernandez-Ruiz J, Romero J, Ramos JA. Endocannabinoids and Neurodegenerative Disorders: Parkinson's Disease, Huntington's Chorea, Alzheimer's Disease, and Others. *Handb Exp Pharmacol*. 2015;231:233-59.
22. Jeon S, Bose S, Hur J, Jun K, Kim YK, Cho KS, Koo BS. A modified formulation of Chinese traditional medicine improves memory impairment and reduces Abeta level in the Tg-APPswe/PS1dE9 mouse model of Alzheimer's disease. *J Ethnopharmacol*. 2011;137(1):783-9.
23. Puzzo D, Lee L, Palmeri A, Calabrese G, Arancio O. Behavioral assays with mouse models of Alzheimer's disease: practical considerations and guidelines. *Biochem Pharmacol*. 2014;88(4):450-67.
24. Prvulovic D, Schneider B. Pharmacokinetic and pharmacodynamic evaluation of donepezil for the treatment of Alzheimer's disease. *Expert Opin Drug Metab Toxicol*. 2014;10(7):1039-50.
25. Kowalska A, Pruchnik-Wolinska D, Florczak J, Modestowicz R, Szczech J, Kozubski W, Rossa G, Wender M. Genetic study of familial cases of Alzheimer's disease. *Acta Biochim Pol*. 2004;51(1):245-

52.

26. Docampo M, Olubu A, Wang X, Pasinetti G, Dixon RA. Glucuronidated Flavonoids in Neurological Protection: Structural Analysis and Approaches for Chemical and Biological Synthesis. *J Agric Food Chem.* 2017;65(35):7607-7623.
27. Van Acker ZP, Bretou M, Annaert W. Endo-lysosomal dysregulations and late-onset Alzheimer's disease: impact of genetic risk factors. *Mol Neurodegener.* 2019;14(1):20.
28. Li LY, Yang CC, Li SW, Liu YM, Li HD, Hu S, Zhou H, Wang JL, Shen H, Meng XM, Li J, Xu T. TMEM88 modulates the secretion of inflammatory factors by regulating YAP signaling pathway in alcoholic liver disease. *Inflamm Res.* 2020;69(8):789-800.
29. Lee B, Sur B, Shin S, Baik JE, Shim I, Lee H, Hahm DH. Polygala tenuifolia prevents anxiety-like behaviors in mice exposed to repeated restraint stress. *Anim Cells Syst.* 2015;19(1):1-7.
30. Sur B, Lee B, Yoon YS, Lim P, Hong R, Yeom M, Lee HS, Park H, Shim I, Lee H, Jang YP, Hahm DH. Extract of polygala tenuifolia alleviates stress-exacerbated atopy-like skin dermatitis through the modulation of protein kinase A and p38 mitogen-activated protein kinase signaling pathway. *Int J Mol Sci.* 2017;18(1):E190.
31. Xin T, Zhang F, Jiang Q, Chen C, Huang D, Li Y, Shen W, Jin Y. Extraction, purification and antitumor activity of a water-soluble polysaccharide from the roots of Polygala tenuifolia. *Carbohydr Polym.* 2012;90(2):1127-31.
32. Kwon KJ, Kim MK, Lee EJ, Kim JN, Choi BR, Kim SY, Cho KS, Han JS, Kim HY, Shin CY, Han SH. Effects of donepezil, an acetylcholinesterase inhibitor, on neurogenesis in a rat model of vascular dementia. *J Neurol Sci.* 2014;347(1-2):66-77.
33. Ogura H, Kosasa T, Kuriya Y, Yamanishi Y. Donepezil, a centrally acting acetylcholinesterase inhibitor, alleviates learning deficits in hypocholinergic models in rats. *Methods Find Exp Clin Pharmacol.* 2000;22(2):89-95.
34. Song, S., Q.F. Liu., M. Hong., G. Kim and B. Koo. In vitro screening of traditional medicinal herbs combined with donepezil for neuroprotective effects in SH-SY5Y cells. *J Oriental Neuropsychiatry.* 2019;30(3):199-207.
35. Zhu Q, Tang CP, Ke CQ, Wang W, Zhang HY, Ye Y. Sesquiterpenoids and Phenylpropanoids from Pericarps of Illicium oligandrum. *J. Nat. Prod.* 2009;72(2): 238-242.
36. Park CH, Choi SH, Koo JW, Seo JH, Kim HS, Jeong SJ, Suh YH. Novel cognitive improving and neuroprotective activities of Polygala tenuifolia Willdenow extract, BT-11. *J. Neurosci. Res.* 2002;70(3):484-492.
37. Lee S, Bang SM, Lee JW, Cho KS. Evaluation of traditional medicines for neurodegenerative diseases using *Drosophila* models. *Evid. Based. Complement. Alternat. Med.* 2014;2014:967462.
38. Devanand DP, Pelton GH, D'Antonio K, Ciarleglio A, Scodes J, Andrews H, Lunsford J, Beyer JL, PEtrella JR, Sneed J, Ciovacco M, Doraiswamy PM. Donepezil Treatment in Patients With Depression and Cognitive Impairment on Stable Antidepressant Treatment: A Randomized Controlled Trial. *Am J Geriatr Psychiatry.* 2018;26(10):1050-1060.

39. Shen L, Liu L, Ji HF. Alzheimer's Disease Histological and Behavioral Manifestations in Transgenic Mice Correlate with Specific Gut Microbiome State. *J Alzheimers Dis.* 2017;56(1):385-90.
40. Shaw KE, Bondi CO, Light SH, Massimino LA, McAloon RL, Monaco CM, Kline AE. Donepezil is ineffective in promoting motor and cognitive benefits after controlled cortical impact injury in male rats. *J Neurotrauma.* 2013;30(7):557-64.
41. Knowles J. Donepezil in Alzheimer's disease: an evidence-based review of its impact on clinical and economic outcomes. *Core Evid.* 2006;1(3):195-219.
42. Sors A, Krazem A, Kehr J, Yoshitake T, Dominguez G, Henkous N, Letondor C, Mocaer E, Béracochéa DJ. The Synergistic Enhancing-Memory Effect of Donepezil and S 38093 (a Histamine H3 Antagonist) Is Mediated by Increased Neural Activity in the Septo-hippocampal Circuitry in Middle-Aged Mice. *Front Pharmacol.* 2016;7:429.
43. Abdel-Salam OM, Youness ER, Morsy FA, Mahfouz MM, Kenawy SA. Study of the effect of antidepressant drugs and donepezil on aluminum-induced memory impairment and biochemical alterations in rats. *Comp Clin Path.* 2015;24(4):847-60.
44. Wolf OT. HPA axis and memory. *Best Pract Res Clin Endocrinol Metab.* 2003;17(2):287–299.
45. Kitraki E, Kremmyda O, Youlatos D, Alexis M, Kittas C. Spatial performance and corticosteroid receptor status in the 21-day restraint stress paradigm. *Ann N Y Acad Sci.* 2004;1018:323–327.
46. Bekris LM, Lutz F, Montine TJ, Yu CE, Tsuang D, Peskind ER, Leverenz JB. [MicroRNA in Alzheimer's disease: an exploratory study in brain, cerebrospinal fluid and plasma.](#) *Biomarkers.* 2013;18(5):455-466.
47. Maes OC, Chertkow HM, Wang E, Schipper HM. MicroRNA: Implications for Alzheimer Disease and other Human CNS Disorders. *Curr Genomics.* 2009;10(3):154-168.
48. Wang P, Liu XM, Ding L, Zhang XJ, Ma ZL. [mTOR signaling-related MicroRNAs and Cancer involvement.](#) *J Cancer.* 2018;9(4):667-673.
49. Cui J, Gong C, Cao B, Li L. [MicroRNA-27a participates in the pathological process of depression in rats by regulating VEGFA.](#) *Exp Ther Med.* 2018;15(5):4349-4355.

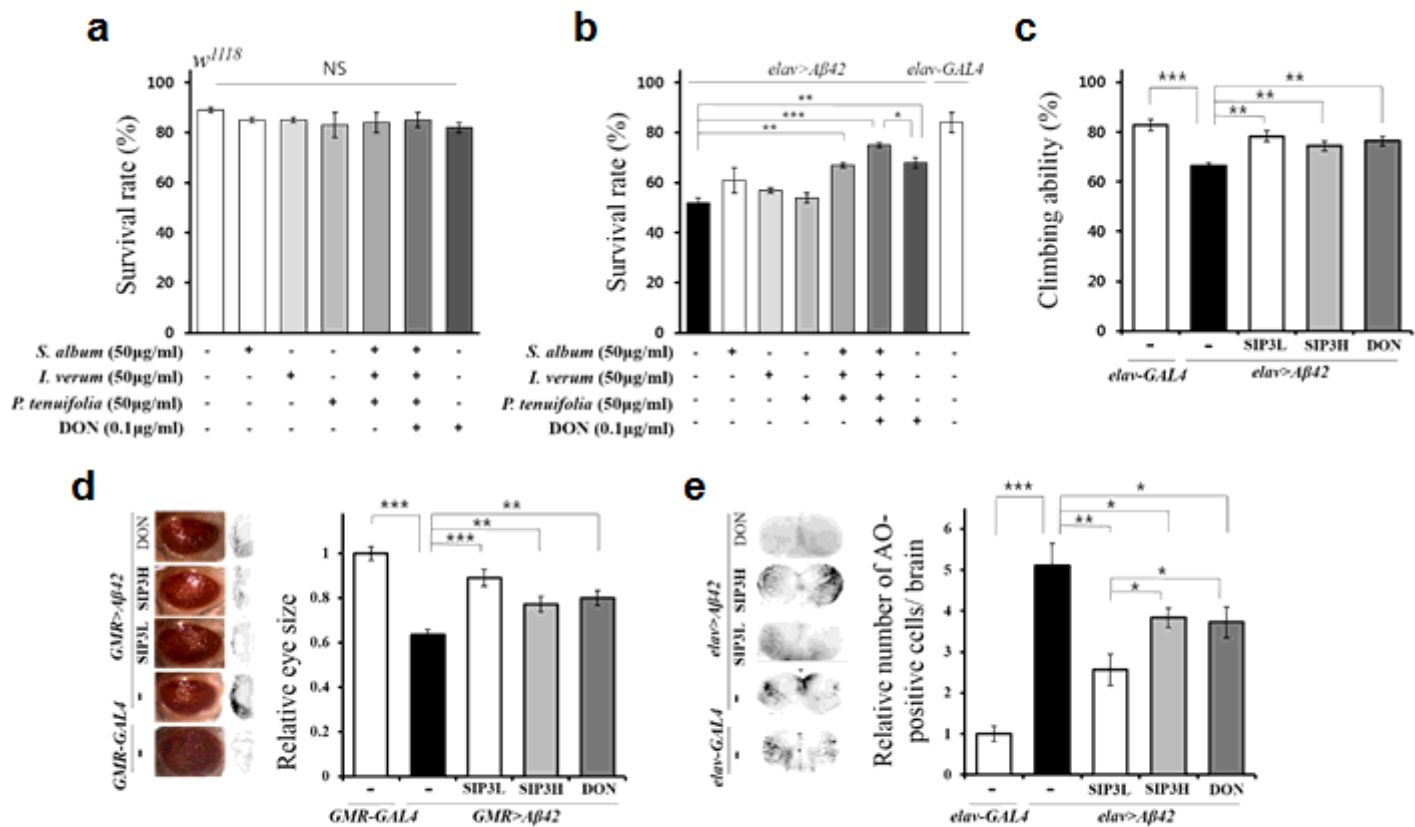
## Table

Table 1

Gene-specific primers used for real-time fluorescence quantitative RT-PCR

Gene name	Forward primer	Reverse primer
Gfap	CGAAGAAAACCGCATCACCA	TGGCAGGGCTCCATTTTCAAT
Il1A	GTCAACTCATTGGCGCTTGA	TGCAAGTTCATGAAGTGAGC
Irs2	CCAACGGGGACTACCTCAAC	ACTGGTCATTGTCTCCGCTG
Nos3	TAGGGCTCGGGCTGGGTTTA	GCTGCCCACTTCCCAATTCT
Tgfb $\beta$ 2	GAGAGGGCGAGGAGTAAAGG	CATTCCACATCCGACTTGGG
Nefh	ACCACCAGGAGGAGGTGG	GTCCAACCTCACTCGGAACC
Gapdh	AGGTCGGTGTGAACGGATTG	TGTAGACCATGTAGTTGAGGTCA

## Figures



## Fig. 1

### Figure 1

SIP3 Extract with donepezil ameliorated A $\beta$ 42-induced survivability, climbing and cell death of Drosophila AD models. (a) The effect of *S. album*, *I. verum*, and *P. tenuifolia* extract separately and also SIP3 or SIP3 with donepezil intake on survivability during wild-type Drosophila development ( $n \geq 200$ ). (b-d) Intake of

*S. album*, *I. verum*, and *P. tenuifolia* extract separately and also SIP3 or SIP3 with donepezil rescued the survivability (b), decreased motor activity (c) and cell death (d) of A $\beta$ 42-expressing flies. All data expressed as the means  $\pm$  SE (\*\*p < 0.001, \*p < 0.01, \*p < 0.05; Student's t-test; b  $\geq$  200; c, n  $\geq$  100; d, n  $\geq$  10). The genotypes of the samples elav>A $\beta$ 42 (UAS-A $\beta$ 42/UAS-A $\beta$ 42; elav-GAL4/ elav-GAL4), GMR-GAL4 (GMR-GAL4/GMR-GAL4), GMR>A $\beta$ 42 (GMR-GAL4, UAS-A $\beta$ 42/GMR-GAL4, UAS-A $\beta$ 42), (SIP3L: co-administration with donepezil and a low 50  $\mu$ g/mL concentration of SIP3 extract; SIP3H: co-administration with donepezil and a high 200  $\mu$ g/mL concentration of SIP3 extract; DON: donepezil alone.)

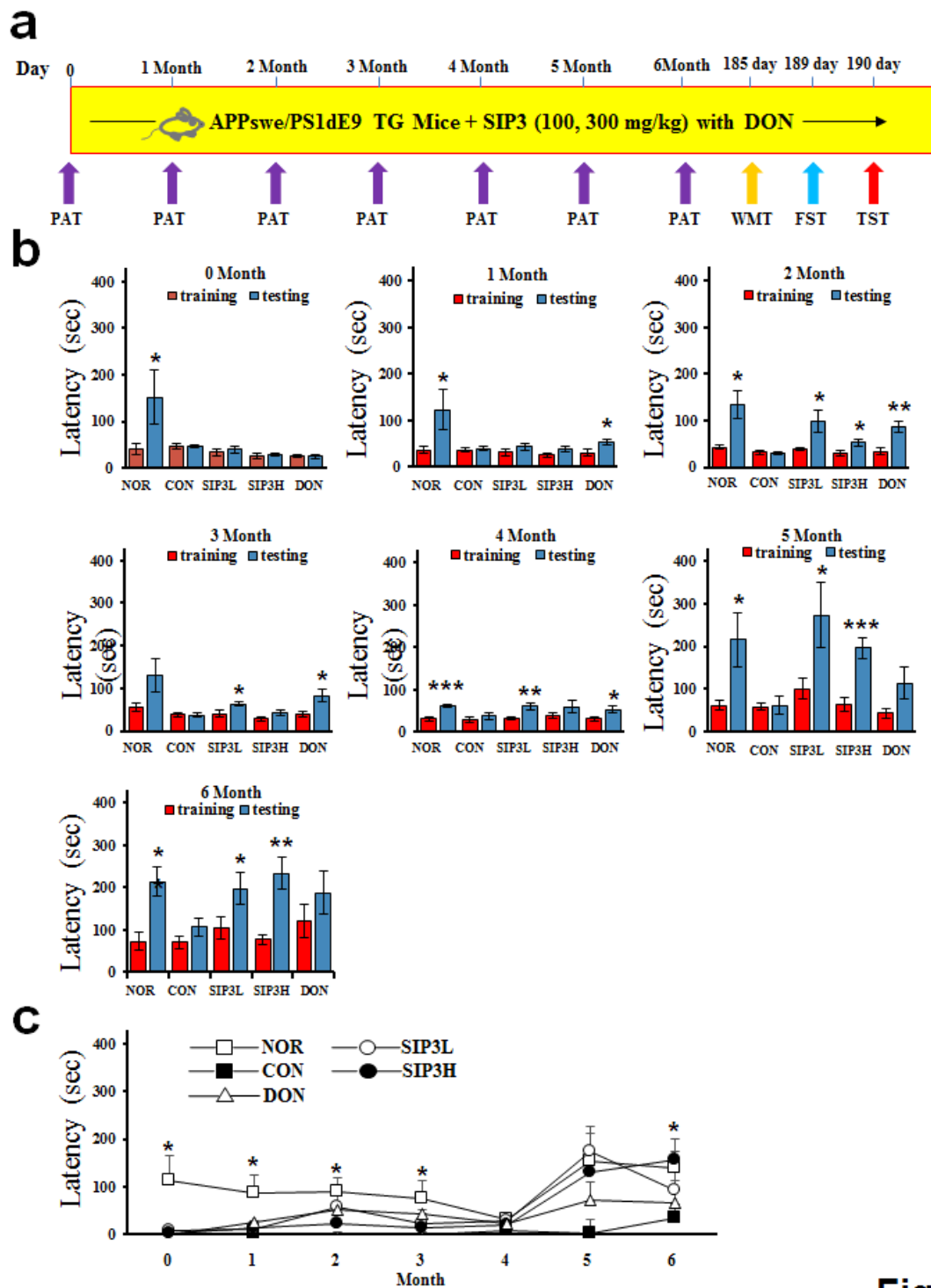


**Fig. 2**

**Figure 2**

Effect of the co-treatment with SIP3 and donepezil on learning and memory impairment of APP/PS1 mice. (a) Schematic drawing of the animal behavior experiments. (b) For the passive avoidance performance test (PAT), mice were trained once and returned to their home cage (training phase). One day after training (testing phase), the average latency time (in seconds) was measured for each group of mice monthly over six months. (c) The change in mean escape latency during the testing phase is shown for

each group. The data are expressed as mean  $\pm$  SEM (n = 5). \*\*p < 0.01, \*p < 0.05 vs. CON. (PAT: step-through passive-avoidance test; MWM: Morris water maze test; FST: forced swimming test; TST: tail suspension test; NOR: normal mice; CON: non-treated APP/PS1 mice; SIP3L: APP/PS1 mice co-treated with donepezil and a low concentration of SIP3 extract; SIP3H: APP/PS1 mice co-treated with donepezil and a high concentration of SIP3 extract; DON: APP/PS1 mice treated with donepezil alone.)

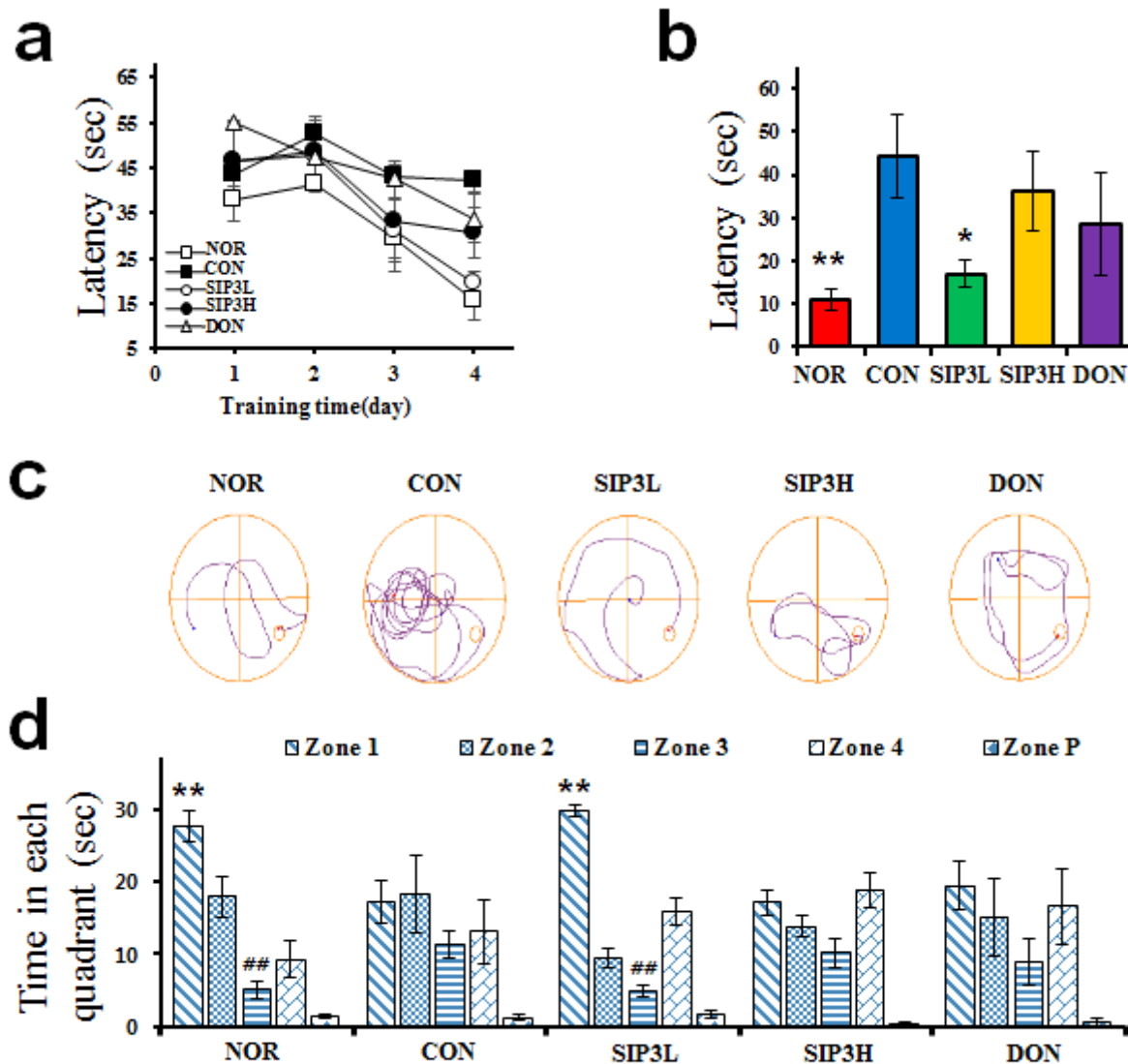


**Fig. 3**

**Figure 3**

Effect of the co-treatment with SIP3 and donepezil on cognitive dysfunction of APP/PS1 mice. The Morris water maze (MWM) test was performed in two phases. The first phase, the training phase (a), was conducted on Days 1-4, and the second, the post-training probe phase (b) was on Day 5 with hidden platform. During the post-training probe phase, spatial learning and memory were significantly improved in the SIP3L mice, compared to those in the CON or DON mice. (c) Search paths from representative mice in different groups. (d) The amount of time spent in each zone was measured over one minute. The data

are expressed as mean  $\pm$  SEM (n = 5). \*\*p < 0.01, \*p < 0.05 vs. CON. (NOR: normal mice; CON: non-treated APP/PS1 mice; SIP3L: APP/PS1 mice co-treated with donepezil and a low concentration of SIP3 extract; SIP3H: APP/PS1 mice co-treated with donepezil and a high concentration of SIP3 extract; DON: APP/PS1 mice treated with donepezil alone.)

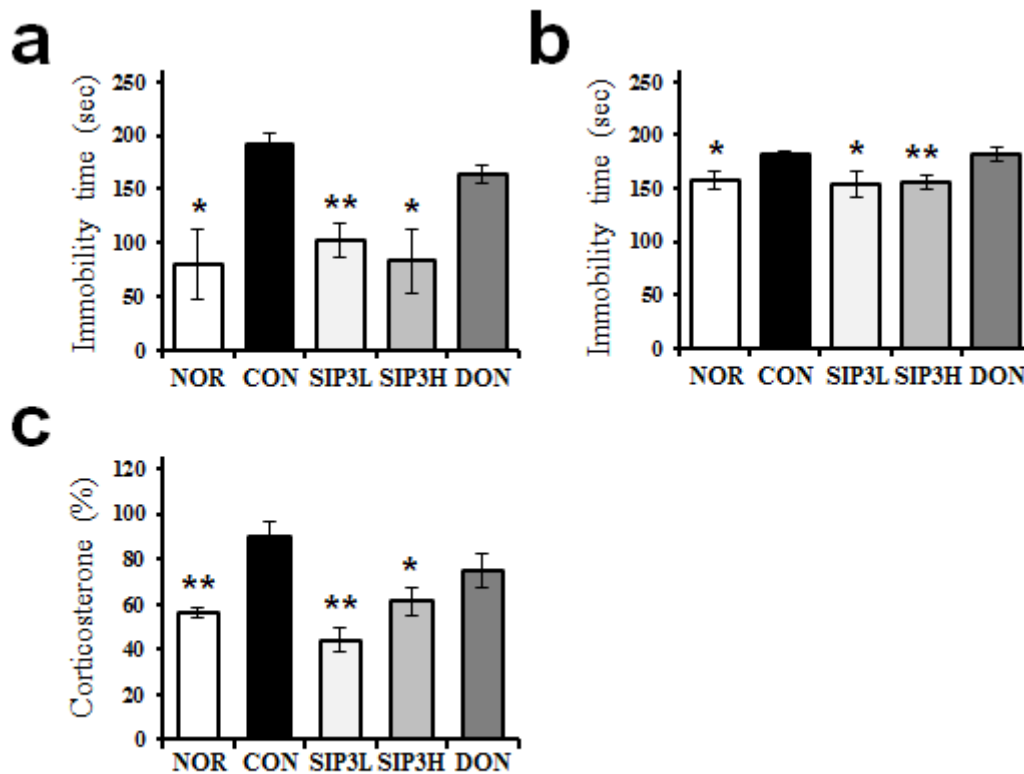


**Fig. 4**

**Figure 4**

Effect of the co-treatment with SIP3 and donepezil on depression-like behavior of APP/PS1 mice. The average immobility time (in seconds) of each group in the forced swimming test (FST; a) as well as tail suspension test (TST; b). (c) Corticosterone levels in serum from each mouse group. The data are expressed as mean  $\pm$  SEM (n = 5). \*\*\*p < 0.001, \*\*p < 0.01, \*p < 0.05 vs. control group. (NOR: normal mice; CON: non-treated APP/PS1 mice; SIP3L: APP/PS1 mice co-treated with donepezil and a low concentration of SIP3 extract; SIP3H: APP/PS1 mice co-treated with donepezil and a high concentration of SIP3 extract; DON: APP/PS1 mice treated with donepezil alone.)

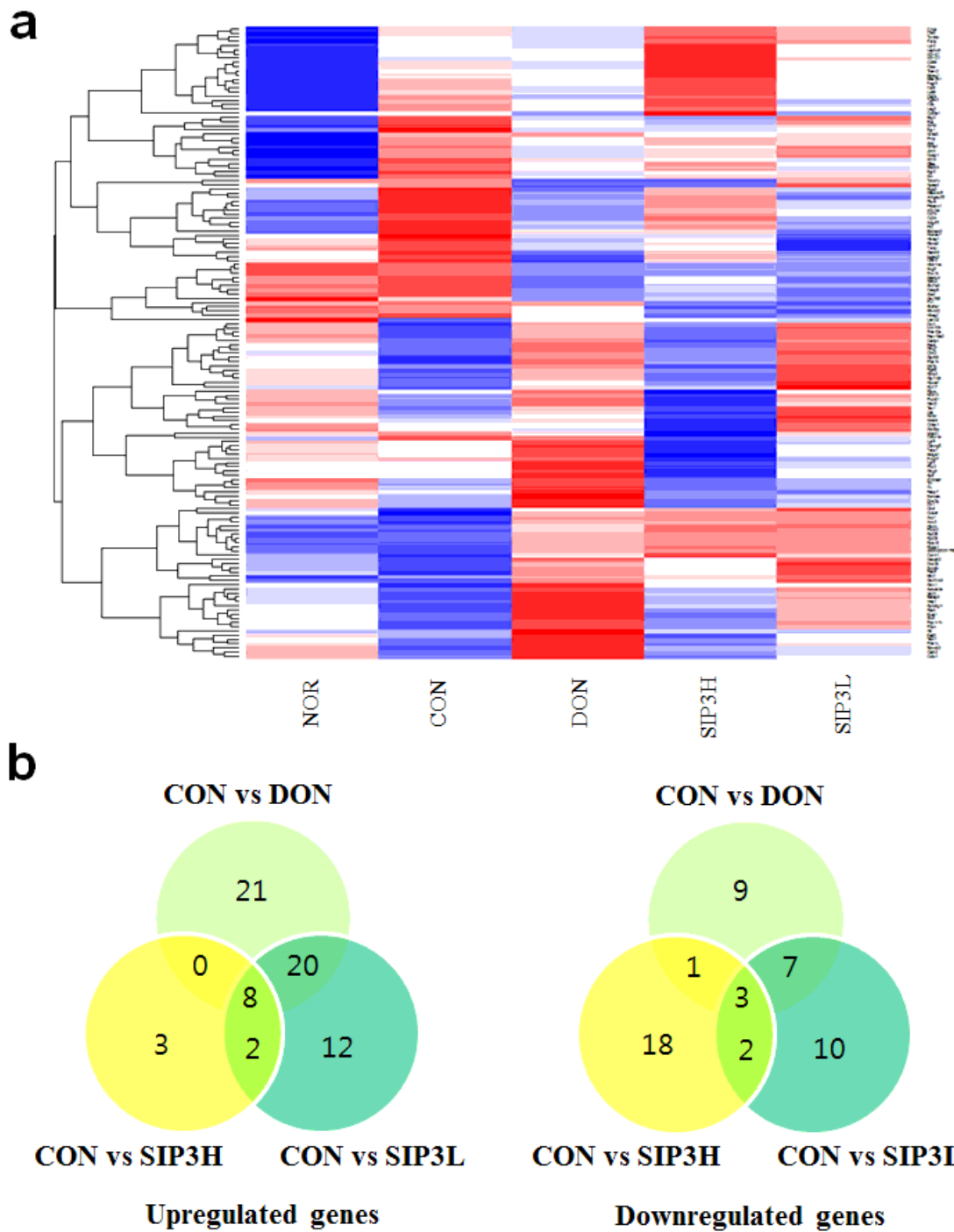


**Fig. 5**

**Figure 5**

RNA-Seq analyses of differentially expressed genes (DEGs) in the cerebral cortex of APP/PS1 mice. (a) Heatmap of the hierarchical cluster analysis of DEGs between samples. Red: upregulated genes; blue: downregulated genes. (b) Venn diagram showing the numbers of upregulated (left panel) and downregulated (right panel) DEGs between groups. Statistically significant DEGs were defined with  $Q$ -value  $< 0.05$  and  $[\log_2FC] > 1.5$  as the cut-off criteria.

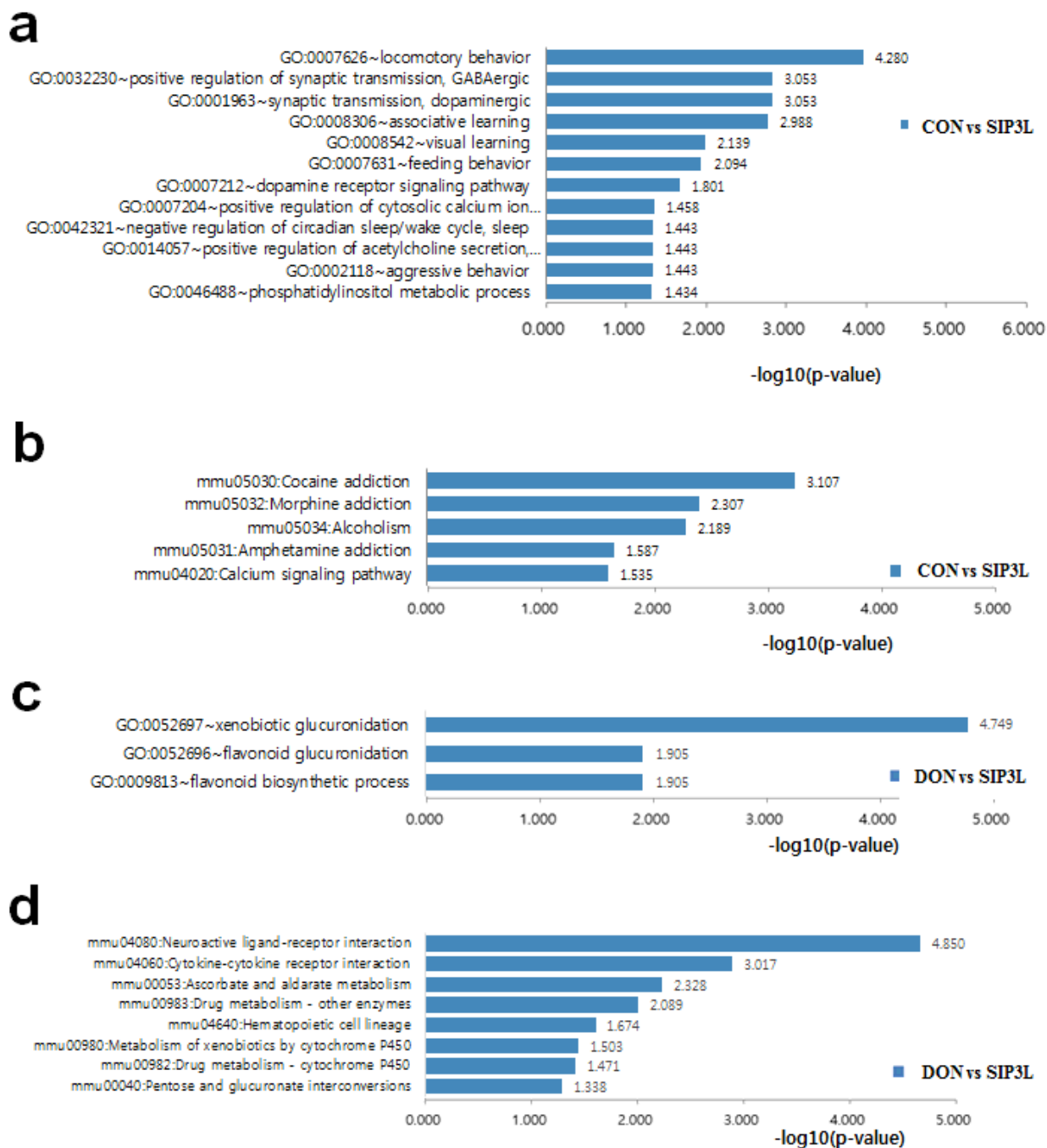


**Fig. 6**

**Figure 6**

GO function and KEGG pathway analysis of DEGs. 1.5-fold change data were evaluated using the Database for Annotation, Visualization as well as Integrated Discovery (DAVID;  $p < 0.05$ ). (a) GO biological processes and (b) KEGG pathway enrichment of DEGs in the cerebral cortex transcriptome in APP/PS1 mice vs CON mice. The horizontal axis represents the  $-\text{Log}_{10}$  (p-value). (c) GO biological processes and (d) KEGG pathway enrichment of DEGs in the cerebral cortex transcriptome in APP/PS1

mice vs DON mice. The horizontal axis represents the  $-\text{Log}_{10}$  (p-value). (GO, gene ontology; KEGG, Kyoto Encyclopedia of Genes and Genomes; DEGs, differentially expressed genes.)

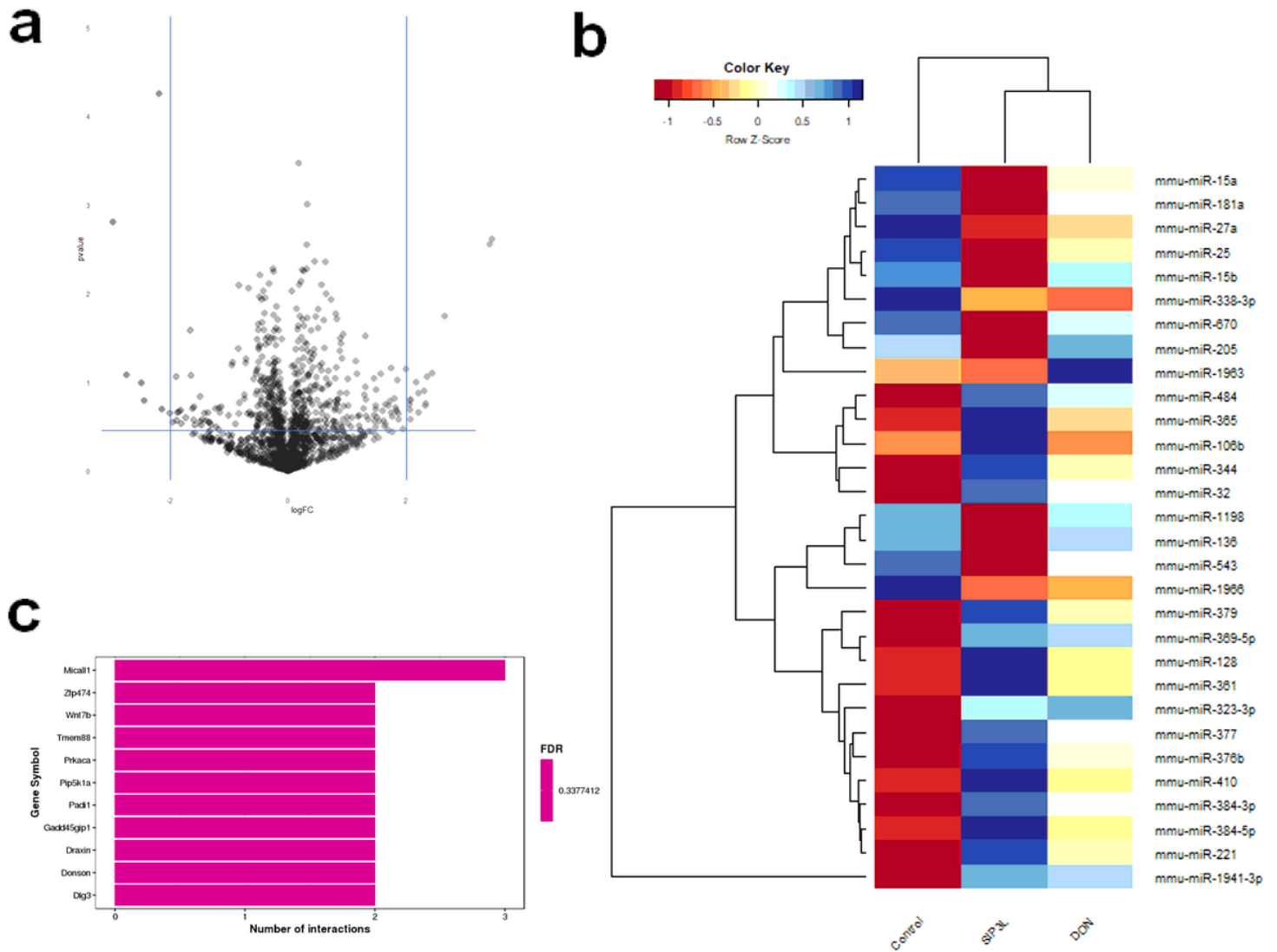


**Figure 7**

miRNA-Seq analyses of differentially expressed miRNAs (DEmiRNAs) in the cerebral cortex of APP/PS1 mice. (a) Volcano plot of miRNA expression. Y-axis represents the P value; X-axis represents the fold-change of each miRNA. (b) Heatmap of the hierarchical cluster analysis of differentially expressed miRNAs between samples with  $P < 0.05$  and  $FC > 2$  cut-off. Red: upregulated miRNAs; Blue: downregulated miRNAs. (c) MiRNA-target Enrichment analysis result. The vertical axis represents the number of interactions between miRNA and target mRNAs.

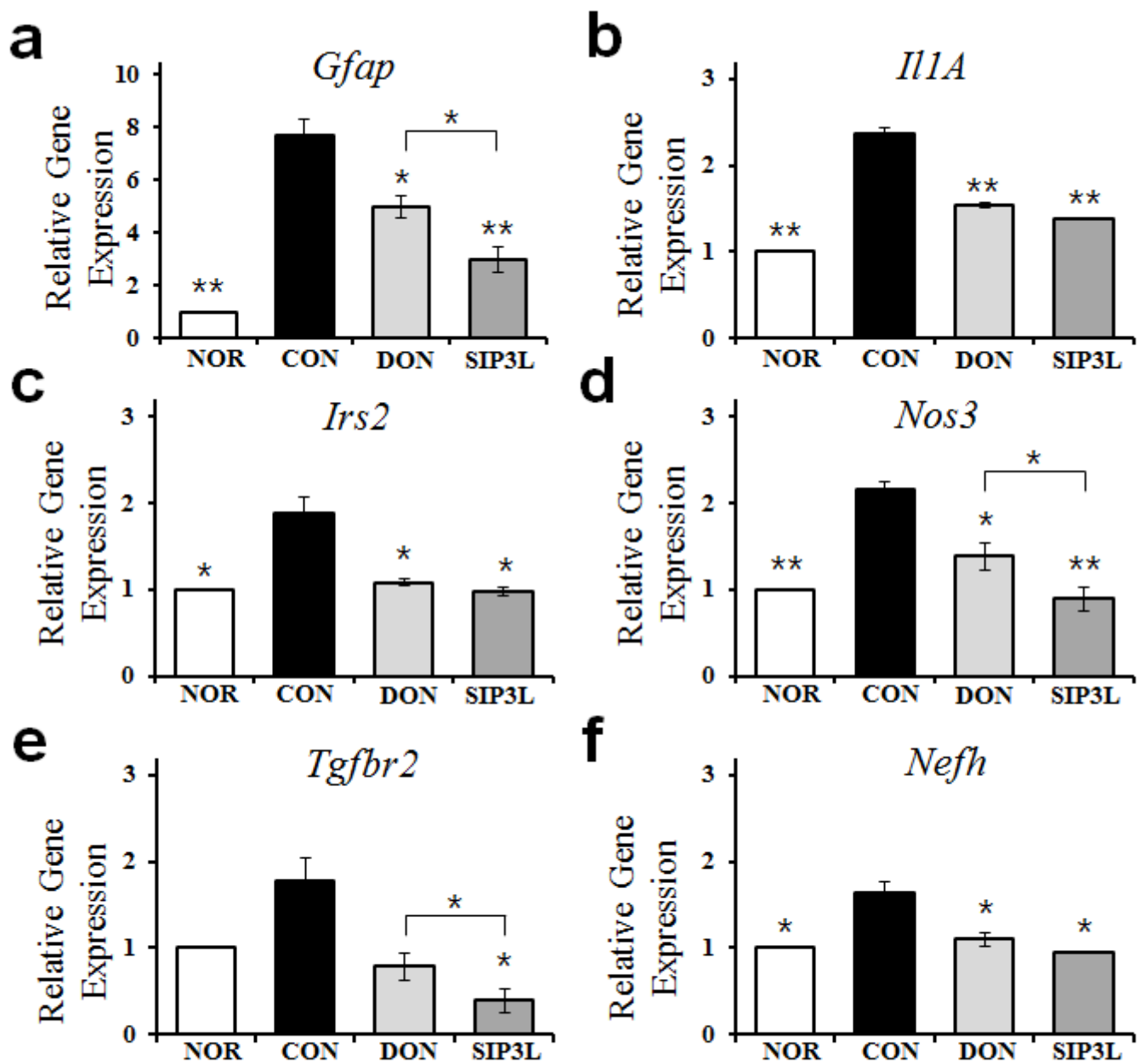


**Fig. 8**

**Figure 8**

qRT-PCR validation of differentially expressed genes identified by deep sequencing. The expression of (a) *Gfap*, (b) *Il1a*, (c) *Irs2*, (d) *Nos3*, (e) *Tgfbr2*, and (f) *Nefh* mRNA. The data are expressed as mean  $\pm$  SEM (n = 3). \*\*p < 0.01, \*p < 0.05 vs. control group. (NOR: normal mice; CON: non-treated APP/PS1 mice; SIP3L: APP/PS1 mice co-treated with donepezil and a low concentration of SIP3 extract; DON: APP/PS1 mice treated with donepezil alone.)

## Supplementary Files

This is a list of supplementary files associated with this preprint. Click to download.

- [Graphicalabstract.tif](#)
- [FigS1.tif](#)
- [FigS2.tif](#)